

High-temperature phase transitions in $K_3H(SO_4)_2$

Calum R.I. Chisholm, Sossina M. Haile*

Department of Materials Science, California Institute of Technology, Pasadena, CA 91125, USA

Received 28 September 2000; received in revised form 13 March 2001; accepted 6 April 2001

Abstract

Two phase transitions in $K_3H(SO_4)_2$ were discovered in the temperature range 25–300°C. The transition temperatures for the mid and high-temperature phases are $T_c = 190^\circ\text{C}$ ($\Delta H = 17.0$ kJ/mol) and $T_c = 227^\circ\text{C}$ ($\Delta H = 7.4$ kJ/mol), respectively, for freshly heated samples. A slow decomposition process begins above 270°C. The conductivity of $K_3H(SO_4)_2$ in these phases ($\sigma = 1.68 \times 10^{-3}$ at 198°C and $2.19 \times 10^{-2} \Omega^{-1} \text{cm}^{-1}$ at 251°C) is comparable to that of other $M_3H(XO_4)_2$ compounds ($M = \text{Cs}, \text{NH}_4, \text{Rb}$ and $X = \text{S}, \text{Se}$) in their superprotonic phases. The activation energy for proton transport in the highest temperature phase of $K_3H(SO_4)_2$ is 0.45 eV, a value slightly higher than in the related compounds. Despite the similarity between the electrical properties of $K_3H(SO_4)_2$ and other $M_3H(XO_4)_2$ compounds, the structural properties are quite distinct. Specifically, high-temperature X-ray powder diffraction measurements show that neither of the high-temperature phases of $K_3H(SO_4)_2$ is trigonal, indeed, the symmetry of the structure decreases at the first transition, in contrast to the superprotonic phases in other $M_3H(XO_4)_2$ compounds. © 2001 Elsevier Science B.V. All rights reserved.

Keywords: $K_3H(SO_4)_2$; Superprotonic phase transitions; $\text{Rb}_3\text{H}(\text{SeO}_4)_2$

1. Introduction

Many compounds in the family $M_3H(XO_4)_2$ ($M = \text{Cs}, \text{NH}_4, \text{Rb}$ and $X = \text{S}, \text{Se}$) undergo a superprotonic phase transition from a monoclinic, pseudo-trigonal, room temperature phase (space group $A2/a$) to a trigonal, high-temperature phase (space group $R\bar{3}m$) [1–3]. For example, $K_3H(\text{SeO}_4)_2$ undergoes such a transition at 117°C [3]. The hydrogen bond network in the high-temperature phase is dynamically disordered, and this feature results in an increase in conductivity by several orders of magni-

tude at the transition. Although $K_3H(SO_4)_2$ is isostructural [4] with other superprotonic members in the $M_3H(XO_4)_2$ family, and thus a similar transition might be expected, its high-temperature properties have not been investigated. In the present work, we demonstrate by thermal analysis high-temperature X-ray powder diffraction, and AC impedance spectroscopy that $K_3H(SO_4)_2$ undergoes two high-temperature transitions, which, despite giving rise to increases in conductivity, are not analogous to those of other $M_3H(XO_4)_2$ compounds.

2. Experimental

Aqueous solutions containing K_2CO_3 and H_2SO_4 were prepared with a molar ratio of $K_2CO_3:H_2SO_4$

* Corresponding author. Fax: +1-626-395-3933.
E-mail address: smhaile@caltech.edu (S.M. Haile).

of 5:16. Single crystals were then grown by slow evaporation of H_2O from the solution under ambient conditions. After 2–8 days, flat, roughly hexagonal plate-like crystals formed at the bottom of the evaporation dishes. Both single crystal and powder X-ray diffraction techniques were used to verify that the crystals were $\text{K}_3\text{H}(\text{SO}_4)_2$. A Siemens D-500 powder diffractometer was employed for X-ray powder analysis ($\text{Cu K}\alpha$ radiation) and single crystal data were collected with a Syntex 4-circle diffractometer ($\text{Mo K}\alpha$ -radiation). High-temperature powder diffraction data were obtained to temperatures of 260°C utilizing an in-house constructed hot-stage, with a temperature stability of $\pm 0.5^\circ\text{C}$ and a temperature accuracy of $\pm 2^\circ\text{C}$.

Thermal analysis was used to detect and characterize high-temperature phase transitions in $\text{K}_3\text{H}(\text{SO}_4)_2$, as well as to establish the material's decomposition temperature. Differential scanning calorimetry (DSC) was performed with a Perkin-Elmer DSC 7 differential scanning calorimeter from 40 to 260°C at a heating rate of $5^\circ\text{C}/\text{min}$ under flowing nitrogen. A Perkin-Elmer TGA 7 was used for thermal gravimetric analysis (TGA). The heating rate was $2^\circ\text{C}/\text{min}$ and the atmosphere, again, flowing nitrogen. Single-crystal samples were employed in both types of thermal analysis.

The conductivities of both single crystals and polycrystalline pellets of $\text{K}_3\text{H}(\text{SO}_4)_2$ were measured using an HP 4284A LCR meter. The applied voltage was 1 V, and the frequency range 20 Hz–1 MHz. The single crystals were polished to ensure opposite surfaces were parallel and to increase the area/length ratio. Polycrystalline pellets were prepared from finely ground single crystals pressed in a 15-mm die under 20 000 lb of pressure for 15 min. Silver paint (Ted Pella, cat no. 16032) was applied on opposite sides of the sample for electrodes. Data were collected on both heating and cooling ($30^\circ\text{C}/\text{h}$) under ambient air atmospheres. Samples were examined over several heating and cooling cycles.

3. Results

The calorimetric measurements (Fig. 1) revealed the presence of two high-temperature phase transitions, at 190 and 227°C . The thermal gravimetric

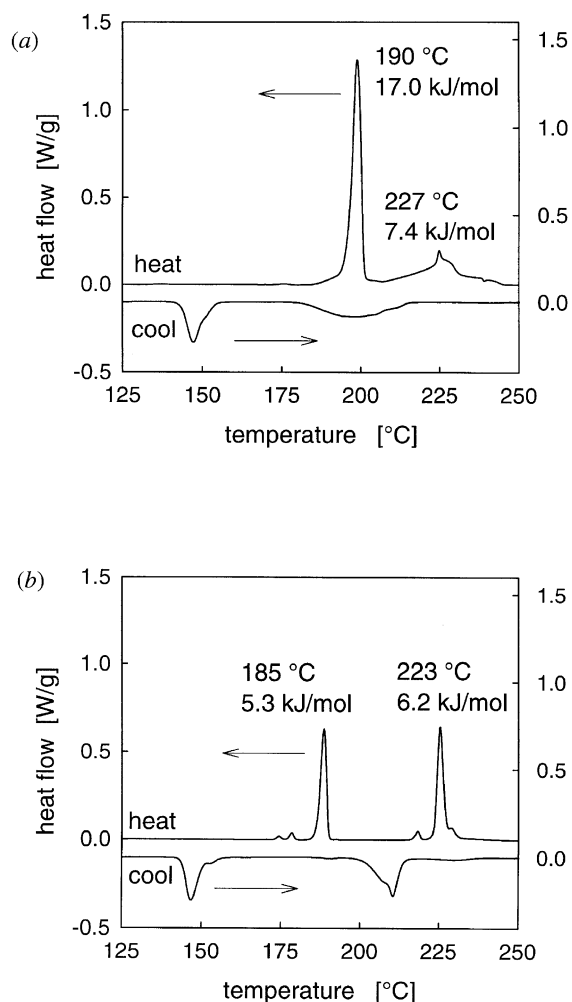


Fig. 1. DSC curves obtained for $\text{K}_3\text{H}(\text{SO}_4)_2$ on both heating and cooling at a rate of $5^\circ\text{C}/\text{min}$ under flowing nitrogen: (a) first heating and cooling cycle, and (b) second heating and cooling cycle, representative of all subsequent cycles.

analysis (Fig. 2) showed that neither transition was due to decomposition; significant weight loss did not occur until $\sim 270^\circ\text{C}$. These results contradict an earlier conclusion reported by Noda et al. [4] that $\text{K}_3\text{H}(\text{SO}_4)_2$ decomposes at $172 \pm 5^\circ\text{C}$. No experimental evidence was provided in support of that conclusion. It is relevant that much slower heating rates (0.5 vs. $2^\circ\text{C}/\text{min}$ as used for the experimental results presented in Fig. 2) led to measurable weight loss in single-crystal samples at lower temperatures, $\sim 250^\circ\text{C}$, and for powdered samples even lower

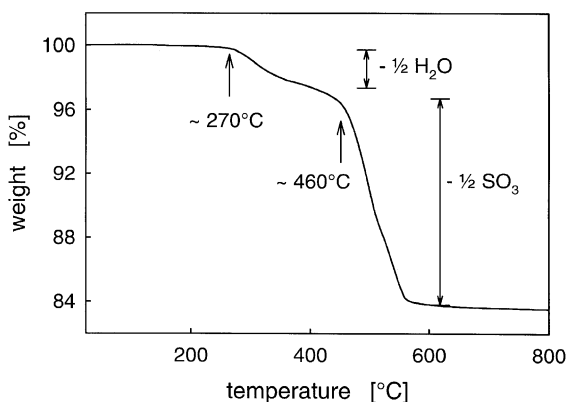


Fig. 2. TGA curve obtained from a finely ground single crystal sample of $K_3H(SO_4)_2$. Significant weight loss begins at $\sim 270^\circ\text{C}$. Sample was heated at a rate of $2^\circ\text{C}/\text{min}$ with nitrogen as the purge gas.

decomposition temperatures were observed. Differences in sample types and heating rates may thus explain the differences between the present and earlier conclusions. Results obtained from single-crystal samples are presented here because they most directly correspond to both the calorimetric and conductivity studies.

The enthalpies of the transitions for a freshly prepared sample (1st heating cycle) were 17.0 and 7.4 kJ/mol, respectively (Fig. 1a). On subsequent heating cycles, the DSC peaks shifted to 185 and 223°C and the enthalpies decreased to 5.3 and 6.2 kJ/mol, respectively. It should be noted that it was necessary to heat samples to temperatures over $\sim 255^\circ\text{C}$ in the first thermal cycle, to obtain reproducible calorimetric results (as shown in Fig. 1b) in subsequent cycles. The difference in thermal behavior between a freshly prepared sample and one already exposed to high-temperatures indicates that the transition from the room temperature monoclinic phase to the high-temperature phase(s) is not reversible (at least on the time scale of the experiment). The sequence of phase transitions is tentatively described as follows:

1st heating cycle $\text{III} \xrightarrow{190^\circ\text{C}} \text{II} \xrightarrow{227^\circ\text{C}} \text{I}$

subsequent cycles $\text{III}' \xleftrightarrow{185^\circ\text{C}} \text{II}' \xleftrightarrow{223^\circ\text{C}} \text{I}$

where II and II' may be the same phase, but III (A2/a) and III' are distinct phases.

The conductivity of $K_3H(SO_4)_2$ is shown in Arrhenius form in Fig. 3. In Fig. 3a, the results for fresh samples measured upon heating (1st heating cycle) are presented, whereas in Fig. 3b, the results for multiply cycled samples measured upon cooling are shown. The two transitions noted by the calorimetric studies for freshly heated samples are evident

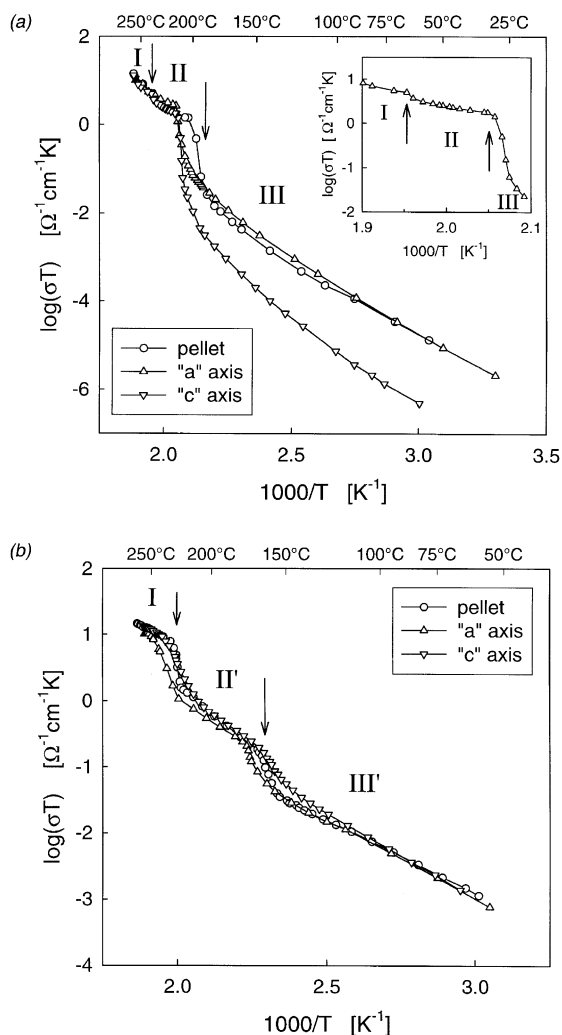


Fig. 3. Temperature dependence of the conductivity of $K_3H(SO_4)_2$ presented in Arrhenius form, $\log \sigma T$ vs. $1000/T$ (heating rate of $30^\circ\text{C}/\text{h}$ and ambient atmosphere): (a) data obtained from the first heating cycle of fresh samples, and (b) data obtained upon cooling samples exposed to multiple thermal cycles. Note the difference in scales.

Table 1

Selected transport properties of $K_3H(SO_4)_2$ Activation energies for proton conductivity determined from a fit of $\sigma = A/T \exp(-E_\sigma/k_bT)$ over the temperature range stated. Conductivity given for the temperature listed. Number in parentheses indicates uncertainty in final digit.

Phase	Measurement	E_σ (eV)	T range (°C)	σ ($\Omega^{-1} \text{ cm}^{-1}$)	T (°C)
III	Pseudo- <i>a</i> , first heat	0.68(1)	40–180	3.13×10^{-6}	130
III	Pseudo- <i>c</i> , first heat	0.87(2)	40–180	1.24×10^{-7}	130
I	Pellet, 'final' cool	0.45(1)	240–255	2.19×10^{-2}	251
II'	Pellet, 'final' cool	0.74(2)	180–210	1.68×10^{-3}	198
III'	Pellet, 'final' cool	0.43(1)	60–140	9.47×10^{-6}	83

from the conductivity data. The first transition leads to a sharp increase in conductivity, whereas the second produces a small, but nevertheless detectable impact on the transport properties (Fig. 3a). Those transitions detected in thermally cycled DSC samples are even more apparent in the conductivity results (Fig. 3b). Much as with the DSC results, it was necessary to anneal samples at temperatures above 255°C for a short period of time to obtain reproducible conductivity data upon cooling. Selected transport properties of $K_3H(SO_4)_2$, corresponding to the results in Fig. 3, are summarized in Table 1.

X-ray powder diffraction patterns of $K_3H(SO_4)_2$ at room and elevated temperatures are presented in Fig. 4. Data were collected at 25, 210 and 248°C after a short anneal at 260°C. In Fig. 4a, these patterns are compared to the as-synthesized and calculated patterns of monoclinic A2/a $K_3H(SO_4)_2$. In Fig. 4b, the high-temperature pattern (248°C) is compared to the calculated pattern for the hypothetical R $\bar{3}$ m phase of $K_3H(SO_4)_2$ (based on the structure determination for $Rb_3H(SeO_4)_2$ [5]) and also that of a hypothetical phase of space group P6 $_3$ /mmc as proposed for $Na_3H(SO_4)_2$ [6]. The lattice constants used for obtaining the calculated patterns were adjusted to the expected unit cell volume of $K_3H(SO_4)_2$ ($a = 5.585$, $c = 7.467$ Å and $a = 5.653$, $c = 21.361$ Å, respectively, for the trigonal and hexagonal phases). Several conclusions can be immediately drawn from the high-temperature diffraction patterns: (1) the structures of the high-temperature phases of $K_3H(SO_4)_2$ are very different from that of the original room temperature phase, (2) accordingly, neither is isostructural with the trigonal superprotonic phase common amongst $M_3H(XO_4)_2$ compounds, and (3) neither is isostructural with the

proposed high-temperature hexagonal phase of $Na_3H(SO_4)_2$.

4. Discussion

The structural phase transition that occurs at 190°C in $K_3H(SO_4)_2$ from the well-known monoclinic phase to an unknown high-temperature phase (phase II) clearly involves dramatic changes in the crystal structure. This is evident not only from the diffraction patterns as discussed above, but also from the magnitude of the enthalpy of the transition (17.0 kJ/mol), which is significantly greater than the enthalpy change associated with the monoclinic to trigonal transition in superprotonic $M_3H(XO_4)_2$ compounds (3–5 kJ/mol) [7,8]. In contrast, phases I, II/II' and III' are all rather similar to one another, as evidenced by the smaller heats of transition (5–7 kJ/mol) for the transformation between these phases, and the similarity of their diffraction patterns. However, it should be noted that despite the similarities of the diffraction patterns there are enough differences, particularly in the region 26–32° 2θ , to support the conclusion from the calorimetric and conductivity measurements that these constitute distinct phases. Unfortunately, none of these patterns could be satisfactorily indexed. The complexity of the high-temperature patterns suggests the unusual result that the symmetry of the compound has in fact decreased upon heating. This is particularly surprising in light of the increase in conductivity upon transformation to the new phase(s). The possibility that the high-temperature diffraction patterns correspond to a multiphase material has been ruled out on the basis of the observation that the patterns were

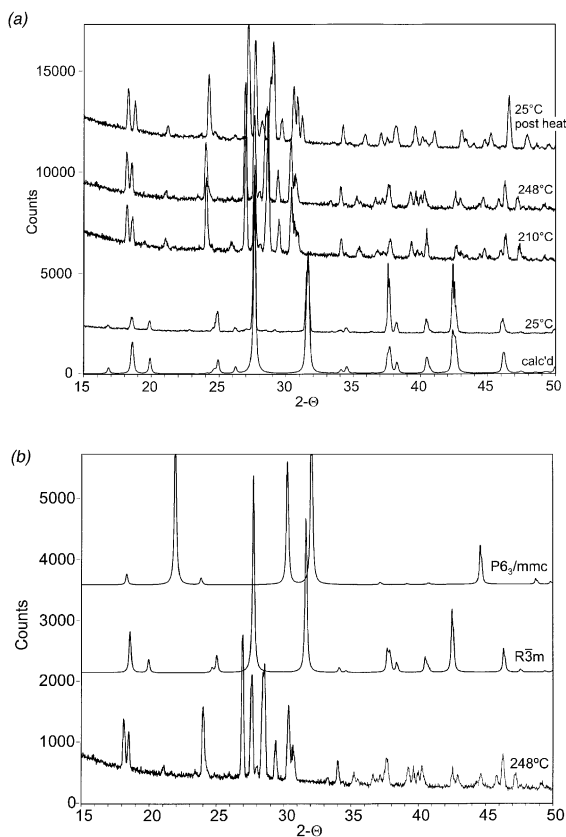


Fig. 4. X-ray powder diffraction patterns of $K_3H(SO_4)_2$: (a) patterns collected at the temperatures indicated after a brief anneal at 260°C and compared to the as-synthesized and calculated patterns of monoclinic $K_3H(SO_4)_2$, and (b) comparison of the pattern of phase I, with the calculated patterns of the hypothetical $R\bar{3}m$ phase of $K_3H(SO_4)_2$, and a hypothetical phase of space group $P6_3/mmc$ as proposed for $Na_3H(SO_4)_2$, as indicated.

highly reproducible from sample to sample, regardless of such details as heating rate and anneal time, without changes in relative intensities between peaks. Furthermore, there was no evidence for the compounds K_2SO_4 or $KHSO_4$ as might be expected for a phase separation/decomposition reaction. Attempts to examine single crystals of $K_3H(SO_4)_2$ by high-temperature diffraction were unsuccessful due to the reduction in crystal quality upon passing through the first phase transition.

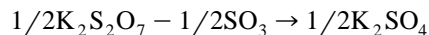
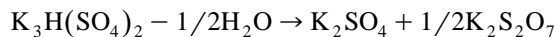
The proton transport properties of $K_3H(SO_4)_2$ in its monoclinic $A2/a$ phase are quite comparable to

those of other $M_3H(XO_4)_2$ compounds [1,2]. The conductivity exhibits significant anisotropy, with transport within the pseudo-(001) plane (along the pseudo- a axis) being significantly more facile than that perpendicular to the pseudo-(001) plane (along the pseudo- c axis). Specifically, the conductivity along the pseudo- a direction is about 30 times greater than that along the pseudo- c direction and the activation energy about 0.2 eV lower (Table 1).

Upon heating to phases II and I, the anisotropy in the conductivity of $K_3H(SO_4)_2$ disappears. This behavior is quite distinct from the other $M_3H(XO_4)_2$ compounds in which the anisotropy is retained in the high-temperature structure [1,2]. The difference again indicates that none of the high-temperature phases of $K_3H(SO_4)_2$ are isostructural with the trigonal phase of the $M_3H(XO_4)_2$ compounds. The apparent isotropy in the conductivity of $K_3H(SO_4)_2$ at high temperature may be due to a truly three-dimensional transport process in a low symmetry phase, or due to a randomization of the crystallographic directions within what has become a polycrystalline sample. The similarity of the conductivities of the polycrystalline pellet and the nominally single-crystal samples (Fig. 3b) are suggestive of the latter. In any case, the high value of the conductivity in phase I, as well as the low value of the activation energy for proton transport ($2.2 \times 10^{-2} \Omega^{-1} \text{cm}^{-1}$ and 0.45 eV, respectively, as determined from the polycrystalline sample upon cooling) earn this phase the title 'superprotonic'. It is noteworthy that phase III', the new room temperature phase obtained after thermal cycling, has a rather low activation energy for proton transport (0.43 eV) and a significantly higher conductivity that the original monoclinic phase ($9.5 \times 10^{-6} \Omega^{-1} \text{cm}^{-1}$ as compared to $4.5 \times 10^{-7} \Omega^{-1} \text{cm}^{-1}$ at 83°C for the polycrystalline pellet). This is perhaps not surprising given the structural similarity between phase III' and the superprotonic phase I of $K_3H(SO_4)_2$.

Turning to the very high-temperature behavior of $K_3H(SO_4)_2$, its decomposition occurs by a two-step process, as evident in Fig. 2. In the first step, which occurs gradually over the temperature range 270–450°C, ~ 3.7 wt.% is lost, corresponding to the loss of 1/2 of a mole of H_2O . In the second step, which takes place from 460 to 580°C, another ~ 13.3 wt.% is lost, corresponding in this case to 1/2 of a mole

of SO_3 . These weight changes can be accommodated by the following reaction sequence,



which imply K_2SO_4 as the final decomposition product at temperatures above 580°C .

5. Conclusions

Several high-temperature phase transitions and new phases were found for $\text{K}_3\text{H}(\text{SO}_4)_2$. Two transitions, which are superprotonic in nature, occur in freshly heated samples at 190°C (III \rightarrow II) and 227°C (II \rightarrow I). In samples annealed briefly at temperatures over $\sim 255^\circ\text{C}$, transitions occur at 185°C (III' \leftrightarrow II'/II) and 223°C (II' \leftrightarrow I), and again, correspond to temperatures at which the conductivity jumps noticeably. Structural rearrangements that occur at the III \rightarrow II transition are severe, involving an enthalpy of transition of 17.0 kJ/mol . None of the new phases, which are rather similar to one another as evidenced by the similarity of their diffraction patterns, are related to the trigonal superprotonic phase encountered in other $\text{M}_3\text{H}(\text{XO}_4)_2$ compounds. Despite the structural similarity of these new phases, significant changes in conductivity occur at the transitions from one to the next, revealing that relatively small structural changes can result in dramatic changes in transport properties. The high-temperature behavior of $\text{K}_3\text{H}(\text{SO}_4)_2$

is particularly unusual in that the compound apparently reduces its symmetry upon heating, yet nonetheless exhibits sharp increases in conductivity. The onset of decomposition occurs at 270°C (for comparable single-crystal samples examined at comparable heating rates) and thus cannot be responsible for the phase transition behavior noted.

Acknowledgements

The authors gratefully acknowledge the financial support of the National Science Foundation and the Irvine Foundation.

References

- [1] A.I. Baranov, A.V. Tregubchenko, L.A. Shuvalov, N.M. Shchagina, *Sov. Phys. Solid State* 29 (1987) 1448–1449.
- [2] A. Pawlowski, Cz. Pawlaczyk, B. Hilczer, *Solid State Ionics* 44 (1990) 17–19.
- [3] S. Yokota, Y. Makita, Y. Takagi, *J. Phys. Soc. Jpn.* 51 (1982) 1461–1468.
- [4] Y. Noda, S. Uchiyama, K. Kafuku, *J. Phys. Soc. Jpn.* 59 (1990) 2804–2810.
- [5] A. Bohn, R. Melzer, R. Sonntag, R.E. Lechner, G. Schuck, K. Langer, *Solid State Ionics* 77 (1995) 111–117.
- [6] R.H. Chen, S.C. Chen, T.M. Chen, *Phase Transit.* 53 (1995) 15–22.
- [7] T. Fukami, H. Ninomiya, R.H. Chen, *Solid State Ionics* 98 (1997) 105–111.
- [8] B. Hilczer, A. Pawlowski, *Ferroelectrics* 104 (1990) 383–388.